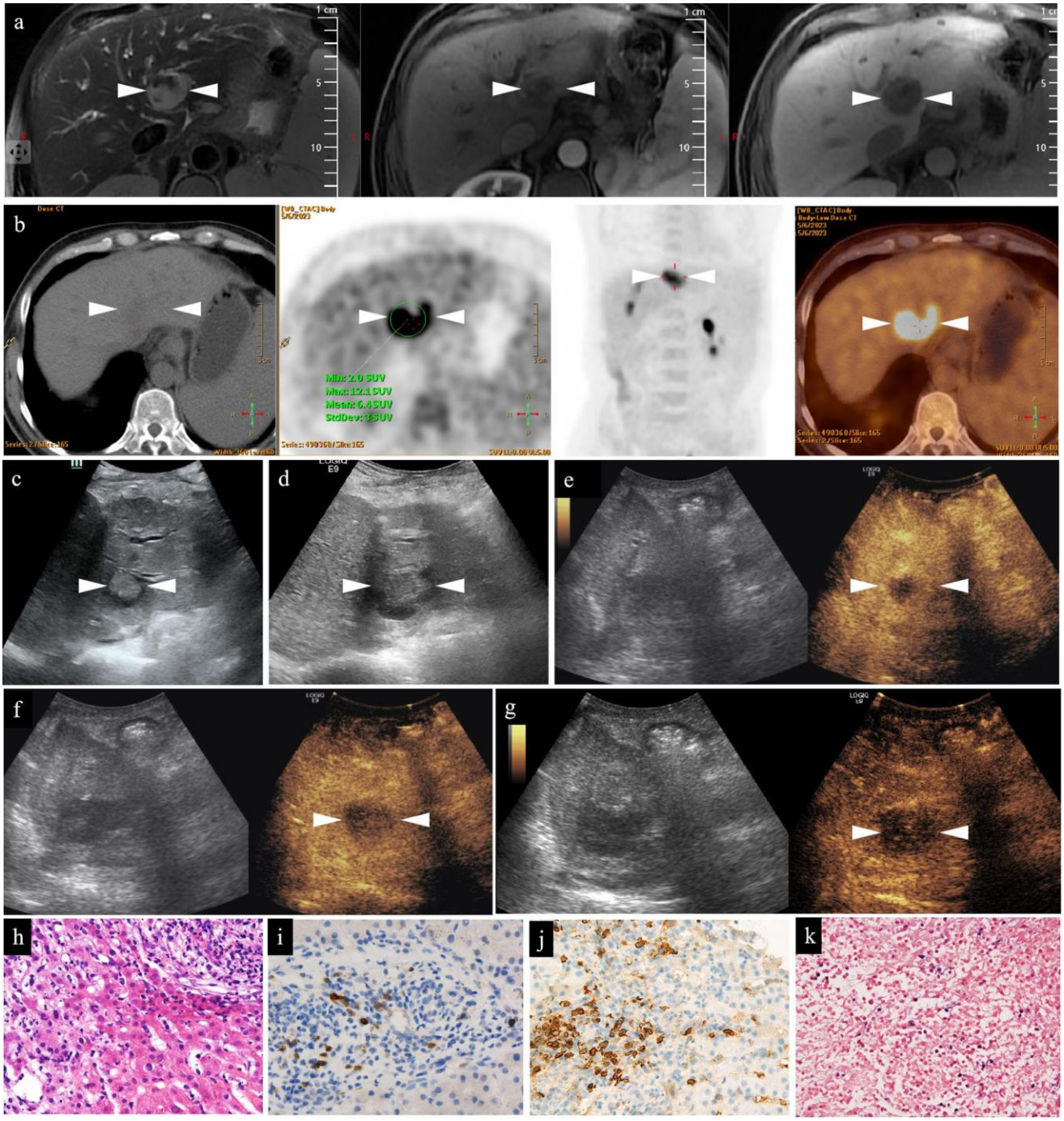

Supplemental Figure S1. Images and histopathological pictures of patient No.1. (a) EOB-MRI. From left to middle to right are HBP, AP, and PP images, respectively. **(b)** Positron emission tomography. In low-density areas of the liver, glucose uptake, which marks the radionuclide 18F-FDG, increased significantly. **(c)** US image when the lesion is first detected (20 mm). **(d)** the US image before biopsy (37mm). **(e)**–**(f)**–**(g)** are CEUS images of the AP, PP, and DP, respectively. **(h–k)** in turn, are histopathological images obtained from biopsied samples of HE, CD19, CD20, and in situ hybridization EBER, respectively (original magnification, ×40). White arrowheads in (a–g) indicate the borders of the lesion.

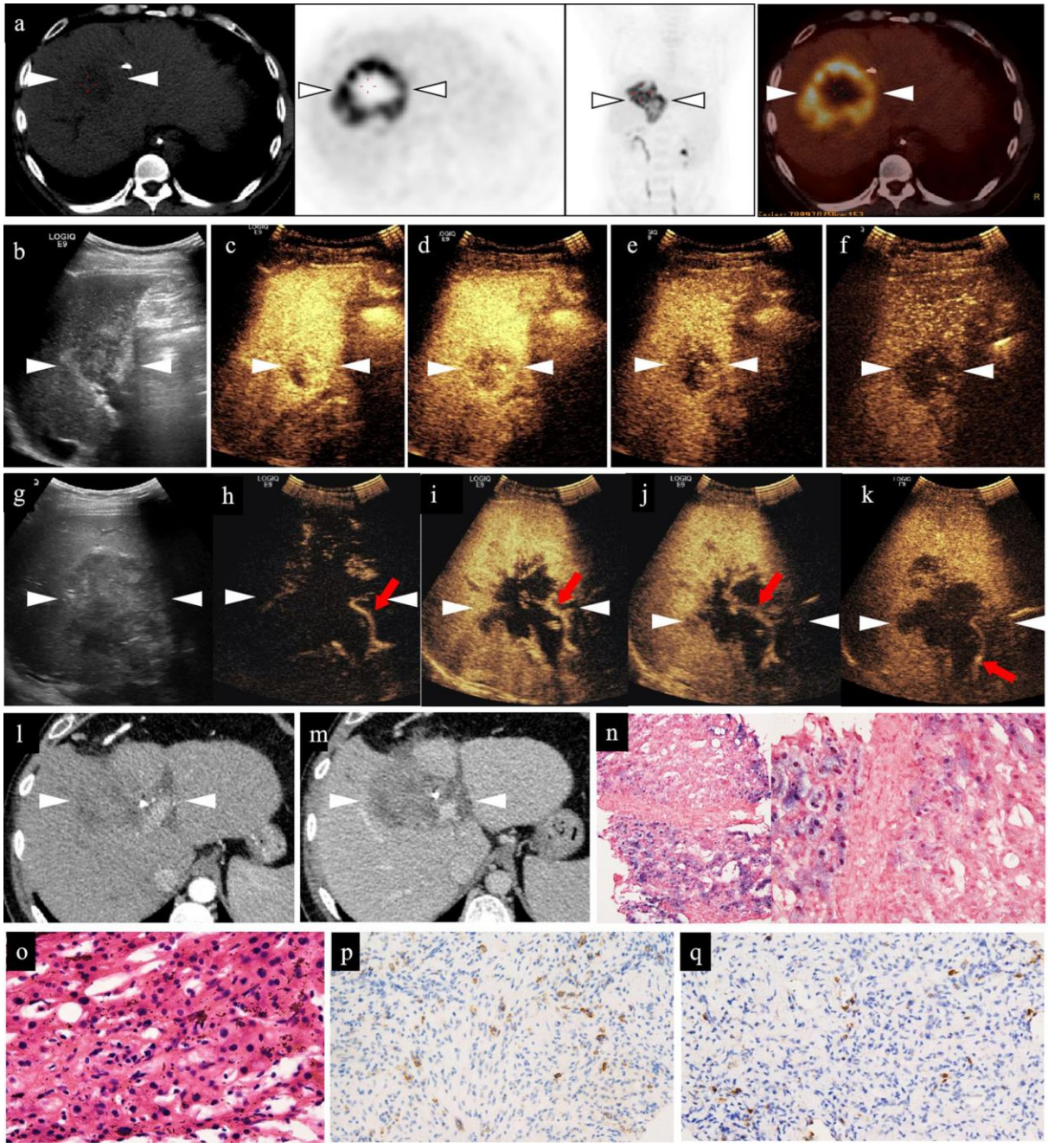

Supplemental Figure S2. Images and histopathological pictures of patient No.2. (a) PET/CT images, suggesting that the activity of glucose metabolism was increased in the hilar lesions. **(b)** US image when the lesion was first detected (27 mm). **(c–f)** CEUS images obtained during early lesion detection. These images are early AP (d), late AP (e), PP (f), and DP (g), respectively. **(g)** US image obtained before biopsy (71 mm). **(h–k)** CEUS images prepared for biopsy. These images are the early AP (h), late AP (i), PP (j), and DP (k). (l) and (m) AP and PP of CECT images, respectively. **(n–q)** are histopathological pictures obtained from biopsied samples of in situ hybridization EBER (n), HE (o), CD19 (p), and CD20 (q), respectively. The left side of picture (n) has original magnification ×10, and the others have original magnifications ×40. White arrowheads in (a–m) indicate the borders of the lesion. The red arrows in (h–k) indicate normal vessels running along the lesion that were not invaded.

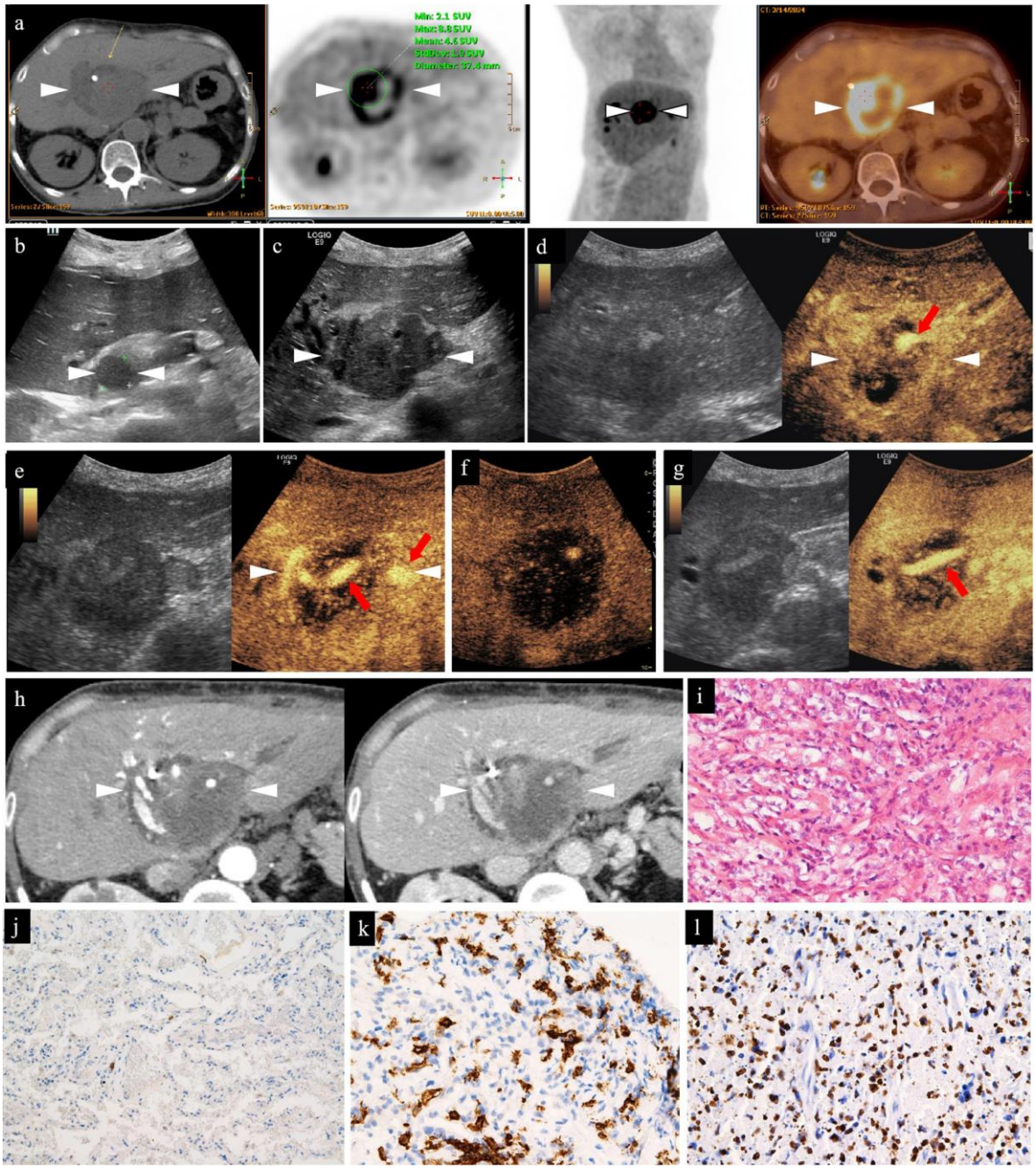

Supplemental Figure S3. Images and histopathological pictures of patient No.3. (a) Positron emission tomography/CT images. The increased inhomogeneous annular glucose uptake in the hilar lesions suggests local necrosis in the center and metabolic activity in the periphery. **(b)** US image when the lesion was first detected (21 mm). **(c)** US image before biopsy (65 mm). **(d–f)** AP, PP, and DP of CEUS images, respectively. **(g)** is also the PP of CEUS, which shows a different scan plane from **(e)**. **(h)** are CECT. The left and right sides show AP and PP images, respectively. **(i–l)** Histopathological images obtained from biopsied samples of HE, CD19 (slightly positive), CD20, and EBER in situ hybridization.(original magnification×40). White arrowheads in **(a–h)** indicate the borders of the lesion. The red arrows in (d), (e), and (g) indicate normal vessels running along the lesion that were not invaded.

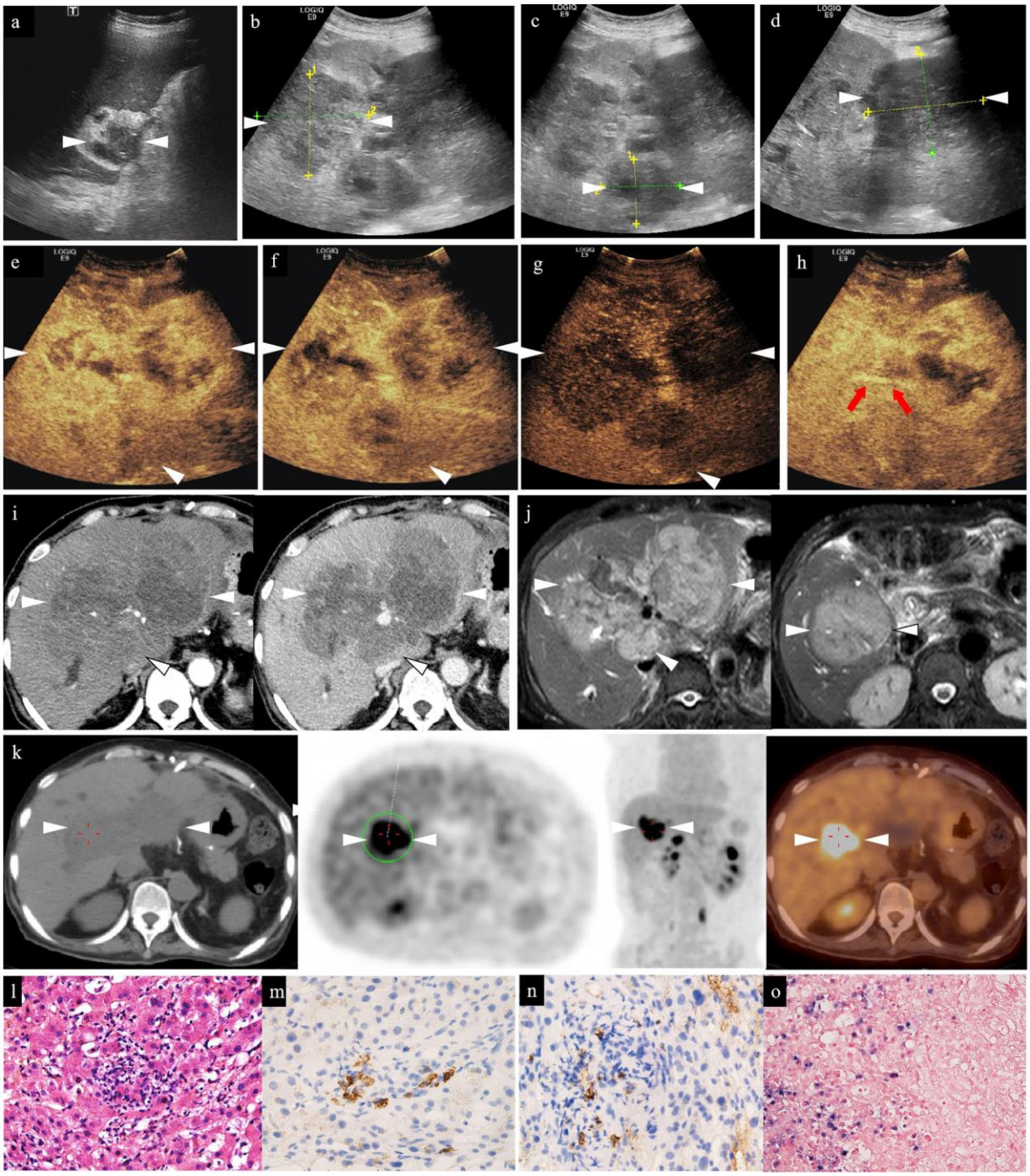

Supplemental Figure S4. Images and histopathological pictures of patient No.4. (a) US image showing a solitary lesion (31 mm) when the lesion was first detected. **(b–d)** US images before biopsy showing multiple lesions close to each other (total measured 149 mm in largest length). **(e–g)** AP, PP, and DP of the CEUS images, respectively. **(h)** is also the PP of CEUS, which shows a different scan plane, as **(f)**. **(i)** are CECT. The left and right sides show the AP and PP images, respectively. **(j)** Images of two different scan planes of the MRCP examination. **(k)** PET/CT images after three cycles of chemotherapy. After chemotherapy, increased glucose uptake was observed in some areas of the lesions. This patient did not undergo pre-treatment PET/CT examination. **(l–o)** are histopathological pictures obtained from biopsied samples of HE, CD19, CD20, and EBER in situ hybridization, respectively. (original magnification×40). White arrowheads in **(a–k)** indicate the borders of the lesion. The red arrows in **(h)** indicate a normal vessel running along the lesion that had not invaded. Because the ultrasound doctors who performed CEUS did not intend to observe the walking vessels at that time, they did not scan the planes with walking vessels specifically, and the images captured from the video of the walking vessel were not clearly shown.

Supplemental Table S1. Immunotherapeutic regimen after liver transplantation

Patient No.	The date of the liver transplant	The regimen of immunosuppressive therapy
No.1	2022.9.2	[After liver transplantation] tacrolimus 1.5 mg Q12h + Meave 720mg Q12h
		[after PTLD diagnosis] anti-CD20 monoclonal antibody Rituximab 660mg (once) + Meave 720mg Q12h + tacrolimus 0.5 mg qd
		[August 3,2023] anti-CD20 monoclonal antibody Rituximab 760mg (once) + Meave 720mg Q12h + tacrolimus 0.5 mg qd
		[August 10,2023, August 17,2023] anti-CD20 monoclonal antibody Rituximab 660mg (once) + Meave 720mg Q12h + tacrolimus 0.5 mg qd
No.2	2021.11.3	[After liver transplantation] Tacrolimus (Henry Pollock)1mg Q12h + mycophenolate mofetil (mycophenolate mofetil)750mg Q12h + methylprednisolone (metformin)8mg Q12h
No.3	2023.6.9	[After liver transplantation] Tacrolimus (Henry Pollock)1.5 mg Q12h + Meave 540 mg Q12h + prednisone 10 mg qd
No.4	2019.4.12	[After liver transplantation]Cyclosporine 200 mg Q12h + mycophenolate Meave 540 mg Q12h + prednisone 10 mg Q12h
		[postoperative fever] Cyclosporine 225mg Q12h + mycophenolate Meave 540mg Q12h + prednisone 10mg Q12h
		[after PTLD diagnosis] Meave 540mg Q12h + prednisone 20mg if necessary
		[2020.6.11] R-CHOP: rituximab 600 mg D 0, Epirubicin 100 mg d 1, vindesine 4 mg d 1, cyclophosphamide 0.8 g, prednisone 100 mg d 1-5）
		[2020.8.16] CHOPD: oxorubicin liposome 40 mg d 1, Ifosfamide 2.5 g d 1, vindesine 3 mg d 1, hydroprednisone 60 mg d 1-5
		[2020.10.13] R-CHO: Prituximab 600 mg D 0, doxorubicin liposome 40 mg d 1, vindesine 4 mg d 1, IFOSFAMIDE 2 g d 1, hydroprednisone 80 mg d 1-5